Progress In Electromagnetics Research B, Vol. 9, 83–96, 2008

ASSESSMENT OF HUMAN HEAD EXPOSURE TO WIRELESS COMMUNICATION DEVICES: COMBINED ELECTROMAGNETIC AND THERMAL STUDIES FOR DIVERSE FREQUENCY BANDS

T. T. Zygiridis and T. D. Tsiboukis

Applied and Computational Electromagnetics Laboratory
Department of Electrical and Computer Engineering
Aristotle University of Thessaloniki
Thessaloniki, 54124, Greece

Abstract—In this paper, an integrated and manifold study of the combined electromagnetic and thermal effects, caused by human exposure to microwave radiation is carried out. In essence, we numerically calculate the amount of electromagnetic power absorbed by biological tissues for various exposure conditions and types of emitting sources, utilizing a detailed model of the human head. The severity of the obtained results is evaluated via comparisons with the guidelines of international safety standards, while further insight is gained by investigating the induced thermal effects. The latter are properly quantified through the solution of the bioheat equation, when combined with the outcome of the electromagnetic simulations. Spatial distributions of the corresponding temperature changes are thus calculated, their relation to the dissipated power is established, and the thermal response of human tissues in marginal cases of exposure is predicted.

1. INTRODUCTION

Human exposure to electromagnetic (EM) radiation, as well as the pertinent health effects, constitute a matter of raised public concern, undergoing continuous scientific investigation. Various studies on this subject exist [1–16], most of which mainly delve into the consequences of mobile-phone usage. Yet, devices and communication terminals operating in other frequency bands have also gained substantial interest in the last years. For example, as wireless networking of computer units is nowadays a rather common trend, the 2 and 5 GHz bands

are intensively utilized for indoor signal transmissions and, therefore, should no longer be overlooked. Regarding physiological effects, local heating of biological tissues is caused by the absorbed EM energy, for which the commonly adopted measure is the specific absorption rate (SAR). The induced temperature changes are currently considered the main source of health risks for the bands examined herein, especially in the case of particularly sensitive organs (such as the brain or the eyes). Protection from potential dangers is based on established safety guidelines [17–19], which propose maximum permissible values for the SAR, in order to exclude or minimize the possibility of overexposure.

This paper aims at providing a thorough description of the effects related to the absorption of EM power by biological tissues, with an emphasis given to the area of the human head. Considering diverse frequency bands (in the range from 900 MHz to 5.8 GHz), as well as radiation conditions (indicating either near- or far-field exposure), SAR values are numerically estimated with the aid of a realistic, highly-detailed computational model. To ensure a generalized framework, our studies encompass transmitting sources in the form of telephone handsets, dipole antennas and propagating plane waves, while consistent evaluation of the results is performed on the basis of international safety regulations. Additional information is acquired by computing the anticipated temperature changes due to EM energy dissipation, and the correlation between averaged SAR indexes and thermal effects is revealed. Other results of critical importance, regarding exposure to conditions that marginally comply with the safety guidelines, are also discussed.

2. METHODOLOGY

2.1. SAR Calculations

As mentioned above, the SAR is the widely accepted means of estimating the absorption of EM power in human tissues (by definition, $\mathrm{SAR} = \sigma E^2/2\rho$, where E is the magnitude of the electric-field intensity, σ the tissue conductivity, and ρ the mass density). Herein, interactions between EM waves and biological matter are reproduced via finite-difference time-domain (FDTD) simulations [20], utilizing an anatomically-based numerical model of the human head, specifically developed for the present study. The head model is reconstructed from two-dimensional MRI data [21], and comprises 24 different types of tissue (fat, muscle, gray and white matter, cortical and cancellous bone, ligaments, skin, mucous membrane, bone marrow, cerebrospinal fluid, cerebellum, glands, lymph, cartilage, blood vessels, teeth, aqueous humor, bodyfluid, blood, nerve spine, sclera, cornea and lens). For

instance, Figure 1 shows a specific MRI image (horizontal slice) together with the part of the corresponding grid realization. The frequency-dependent electrical properties of the tissues are determined from the parametric models of [22]. For our needs, the overall size of the computational domain is $228 \times 272 \times 301$ cubic Yee cells with 1-mm sides, enclosed by a six-cell perfectly matched layer [23] for outgoing-wave cancellation. Note that maintaining an adequate level of spatial resolution and detail is of critical importance in bioelectromagnetic simulations, as oversimplifications are prone to erroneous calculations [7].

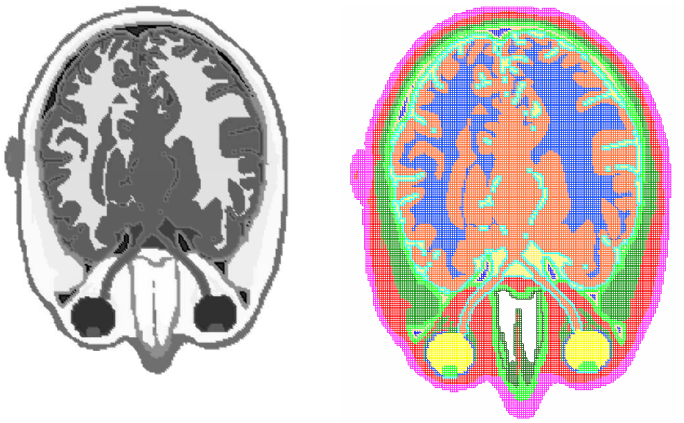

Figure 1. An MRI image (left) and the corresponding FDTD grid (right) for a horizontal slice.

The SAR is determined in the center of each cell after steady state has been established, by taking into account the average of the twelve surrounding electric components. In a post-processing stage, volume averaging (which is required by contemporary safety standards) is performed within cubes containing 10 g of tissue (this index is labeled SAR-10g). We also calculate SAR*-10g in the same manner, but with the additional constraint that air should not occupy more than 20% of the cubical volume. Apparently, it is expected that SAR*-10g $<$ SAR-10g, due to the exclusion of superficial points. In addition, SAR-1g values, extracted from cubes containing 1g of tissue, are also obtained for comparison purposes (this measure was utilized by the older IEEE standard [19]).

2.2. Safety Standards

The suitability of wireless devices — with respect to health issues — is mainly quantified via their compliance with the established safety guidelines, in terms of the volume-averaged SAR. Specifically, ICNIRP [17] proposes a 10 g-averaged SAR value of 2 W/kg at most, for general public exposure. Up to 3 GHz, the 2005 revision of the IEEE standard [18] has the same SAR limits as ICNIRP in the head region, except for the case of the pinna, where the SAR limit is 4 W/kg. The former 1999 IEEE standard [19] followed a different direction, as it limited the maximum SAR-1g value to 1.6 W/kg in uncontrolled environments. According to a recent study [13], the revised IEEE version appears to be more relaxed, not only compared to the older one, but also to the ICNIRP regulations.

2.3. Thermal Simulations

After SAR has been calculated and recorded, it is utilized as the source term in the transient bioheat equation [3, 5, 13, 14, 24],

$$\begin{aligned} &\nabla \cdot \left(K\left(\mathbf{r}\right) \nabla T\left(\mathbf{r},t\right)\right) + \rho\left(\mathbf{r}\right) \mathrm{SAR}\left(\mathbf{r}\right) + Q\left(\mathbf{r}\right) \\ &-B\left(\mathbf{r}\right)\left(T\left(\mathbf{r},t\right) - T_b\right) = C(\mathbf{r})\rho\left(\mathbf{r}\right) \frac{dT\left(\mathbf{r},t\right)}{dt} \end{aligned} \tag{1}$$

whose solution provides the desired thermal response. In (1), T and T_b denote tissue and blood temperatures, respectively, K is the tissue thermal conductivity, B is associated with blood flow, C is the heat capacity, and Q represents heat sources due to metabolic processes. Furthermore, variables $\mathbf{r}$ and t indicate the spatial and temporal dependence of the various quantities. Special treatment is called for air-tissue interfaces, according to the boundary condition

$$K\left(\mathbf{r}\right) \frac{\partial T\left(\mathbf{r},t\right)}{\partial n} = -H\left(T_s\left(\mathbf{r},t\right) - T_a\right) \tag{2}$$

where T_s and T_a are the surface and air temperatures, respectively, and H stands for the convection coefficient. In all cases we have considered $T_b = 37$ °C, and $T_a = 23$ °C, while the various thermal parameters have been chosen according to data taken from the relevant literature (e.g., [3, 13]). The solution of (1) is calculated with a conditionally-stable FDTD scheme [5], simulating 30 min of actual exposure (after this period, no significant thermal changes are expected). The necessary initial conditions ($T\left(\mathbf{r},0\right)$) are also determined from (1), assuming total absence of external heat sources (i.e., $\mathrm{SAR}(\mathbf{r}) = 0$).

3. RESULTS

3.1. Radiation from Mobile Phones

For this type of studies, generic models of mobile phones have been developed and applied, with dimensions $4.8 \times 1.9 \times 12.5$ cm. In fact, two different versions are implemented (for 900 and 1800 MHz), integrating antennas similar to those described in [25] for the aforementioned bands (Figure 2). To ensure proper functionality, additional simulations of the handsets operating in free space, have confirmed the efficient operation of the integrated radiating elements, with respect to the return loss. We place the devices adjacent to the ear and examine two different orientations (0° and 30° tilt angles, with respect to the vertical direction), to simulate typical use. Note that the level of the output power is set to 0.25 W at 900 MHz, and 0.125 W at 1800 MHz.

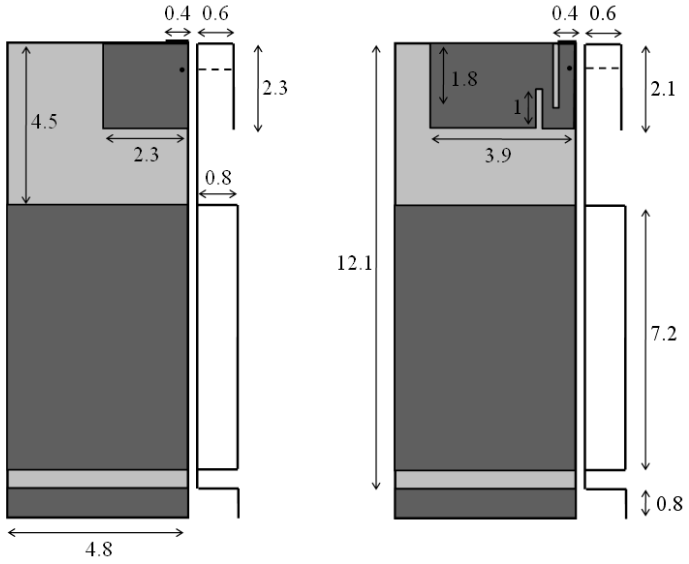

Figure 2. Geometric configuration of the modeled handsets, at 900 MHz (left) and 1800 MHz (right). All dimensions are given in cm.

Figure 3 displays the distribution of the normalized SAR when the mobile phones are vertically aligned, where the weaker penetration at the higher band is evident. Next, some more general results are summarized in Table 1, regarding the volume-averaged SAR and the corresponding temperature elevations. It can be seen that there is a non-trivial safety margin for SAR-10g, when compared to either the

ICNIRP or the IEEE-2005 guidelines, since the maximum values are found less than 1 W/kg. Therefore, taking into account the safety limits, output power levels that are at least two times higher than the considered ones seem to be permissible. SAR*-10g appears lower than SAR-10g, due to the unavoidable exclusion of nodes close to the surface, with their maximum difference being approximately 19%. On the other hand, the peak values of SAR-1g may lead to different conclusions, as they are comparable to (or slightly greater than) the IEEE-1999 limit of 1.6 W/kg, thus verifying the more relaxed character of the newest version.

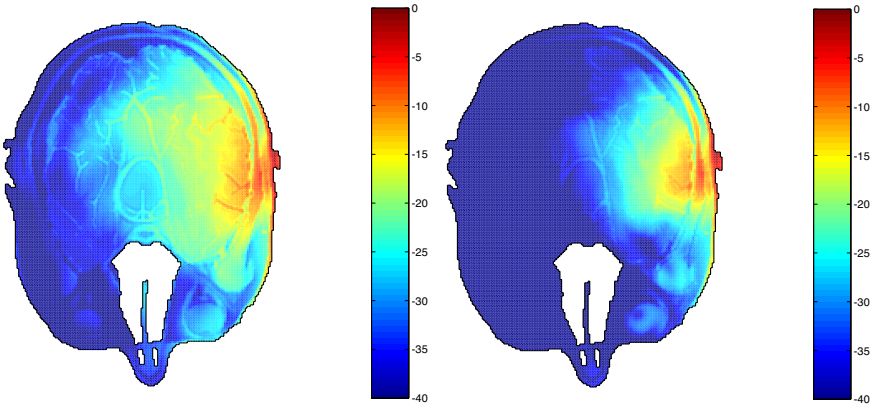

Figure 3. Normalized SAR distributions (dB) from a vertically-aligned mobile phone, operating at (a) 900 MHz and (b) 1800 MHz.

Note that, due to the radiators' proximity to the head, our calculations indicate that a significant amount of EM power is coupled to the tissues, rather than radiated. Specifically, this percentage reaches 68.4% at 900 MHz and 53.78% at 1800 MHz. Regarding the induced thermal effects, it is found that peak temperature elevations ΔT are rather small (within the range 0.08–0.12°C) and observed in the skin. The changes in the brain area (ΔT_{br}) can be considered negligible as well, since they are lower than 0.06°C. To elaborate further, Figure 4 exhibits the levels of these increases, as ones moves from outer toward internal points. The 1800-MHz case clearly exhibits a more rapid spatial weakening of the thermal alterations, owing to the superficial character of energy deposition.

Table 1. Maximum SAR values (W/kg) and peak temperature changes (°C) for the case of mobile phones.

Case	SAR-10g	SAR*-10g	SAR-1g	ΔT	$\Delta T_{\rm br}$
900 MHz (0°)	0.840	0.752	1.293	0.098	0.053
900 MHz (30°)	0.789	0.775	1.140	0.078	0.043
1800 MHz (0°)	0.853	0.757	1.571	0.110	0.045
1800 MHz (30°)	0.963	0.778	1.627	0.115	0.039

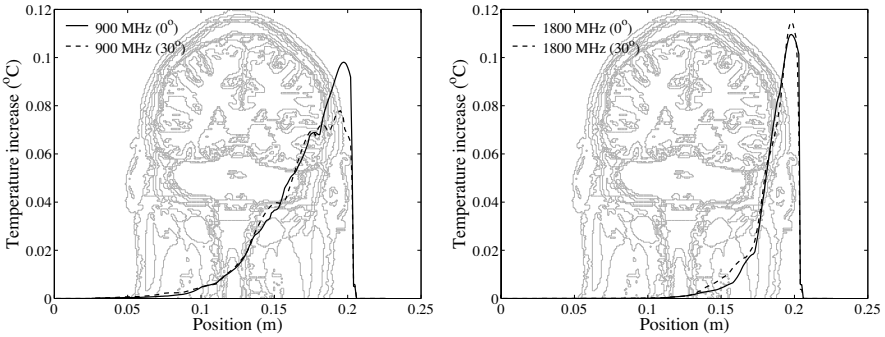

Figure 4. Maximum temperature changes observed within vertical slices, for different handset orientations and frequency bands.

3.2. Emissions from Dipole Antennas

To further investigate local absorption phenomena, the present study also incorporates simulations of exposure to vertically-aligned, half-wavelength dipole antennas, when placed closely to the human head. Specifically, the radiators' positions are chosen near to either the ear (case I) or the eye (case II). The latter case is of special interest, because eyes are considered quite sensitive organs, due to their low level of blood flow (which is a primary cooling mechanism). Overall, four frequency bands are examined (900 MHz, 1800 MHz, 2.44 GHz and 5.8 GHz), with the levels of the output power selected equal to 250, 125, 100, and 100 mW, respectively.

The dissipated power as a function of the distance from the head is drawn in Figure 5 for various configurations. Evidently, despite the relatively low energy content of the radiated waves, it can be seen that significant values of the averaged SAR are calculated, due to the small head-antenna separation. Especially in case I, the 2 W/kg limit

(but not the IEEE pinna limit) is found to be violated for certain antenna positions. The highest SAR-10g values for the four bands are 1.447, 2.178, 2.802, and 2.29 W/kg (case I), and 1.217, 1.765, 1.756, and 1.677 W/kg (case II), respectively. On the other hand, the most prominent temperature changes are found to lie between 0.156 and 0.406°C in case I, while the corresponding range in case II is 0.198–0.484°C. As previously, milder thermal effects occur in the brain area; the most notable change is observed in case II at 1800 MHz, and it is approximately 0.117°C.

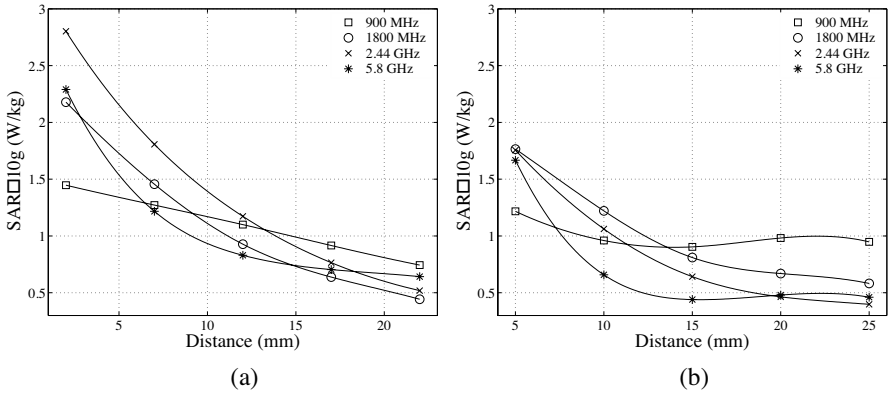

Figure 5. SAR-10g versus head-antenna separation, when dipole antennas are placed adjacent to (a) the ear, and (b) the eye.

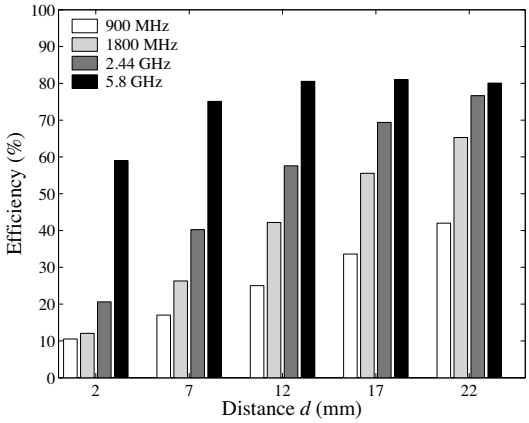

Figure 6. Antenna efficiency (%) of dipole antennas, for various operating frequencies and placements, next to the ear.

The amount of power that is absorbed by human tissues is also found to be different in each frequency band, as deduced from Figure 6, where the antenna efficiency is exhibited for case I. Clearly, a smaller head-dipole distance implies more severe energy absorption, especially at larger wavelengths.

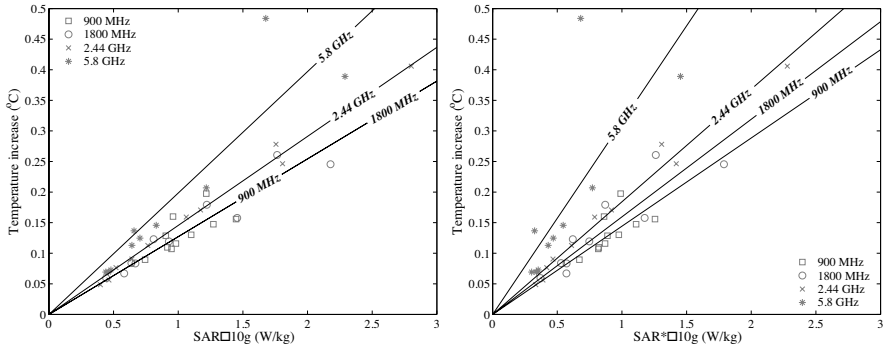

Figure 7. Maximum temperature elevations versus peak SAR-10g and SAR*-10g, for the case of dipole antennas.

Next, all the induced temperature changes are given in the scatter plot of Figure 7, as functions of the peak SAR-10g and SAR*-10g. In addition, regression lines that match the given data in a least-squares manner are drawn. These lines comply with the simple formulas $\Delta T \simeq a\times$SAR-10g, and $\Delta T \simeq a^*\times$SAR*-10g, since no thermal alterations are anticipated in the absence of dissipated power. Table 2 refers to the calculated slopes of the regression lines for each band; a general approximation, derived from the total of the numerical data, is also considered. For comparison and validation, the following similar results from other published studies can be taken into account:

- Values between 0.185 and 0.237 were calculated for a in [6], where several simulations in the band 900 MHz–2.45 GHz were performed.
- In [13], it was found that $\Delta T \simeq (0.1044 \pm 0.0192)\times$SAR-10g at 835 MHz, or $\Delta T \simeq (0.0.0886 \pm 0.0078)\times$SAR-10g at 1900 MHz, considering non-pinna tissues. These results relied on various mobile phone and head models.
- In [14], the slope of the regression lines ranges from 0.113 to 0.165, referring to two head models, and frequencies from 900 MHz to 2.45 GHz.

In addition, the expected temperature elevations when the common 2 W/kg limit is reached are also mentioned in Table 2.

Apparently, thermal changes larger than 0.4°C are unlikely to take place. Similar estimations can be obtained for controlled (occupational) exposure as well, where five-time larger temperature increases should be expected.

Table 2. Slope of the least-squares regression lines and maximum temperature increases at the 2 W/kg limit.

Case	a	$\Delta T_{2\,\mathrm{W/kg}}$	a^*	$\Delta T_{2\mathrm{W/kg}}$
900 MHz	0.12712	0.25	0.14423	0.29
1800 MHz	0.12718	0.25	0.15954	0.32
2.44 GHz	0.14554	0.29	0.18417	0.37
5.8 GHz	0.19853	0.40	0.31452	0.63
Overall	0.14861	0.30	0.18384	0.37

Interestingly, the mass of the eyeball is approximately 8.15 g, i.e., close to 10 g. Therefore, SAR averaged over the eye's volume can serve as a consistent estimator. For the frequency bands of case II, peak SAR-eye indicators reach 0.584, 1.042, 0.733 and 0.099 W/kg, respectively, with the most prominent ΔT being equal to 0.198°C.

3.3. Far-Field Exposure

We now pay attention to the case of exposure at maximum allowable power levels, as those are dictated by the safety standards. The excited EM fields are selected to have plane-wave forms, impinging on the human head at angles from $-90°$ to $90°$, at two wireless networking frequencies (angles are determined with respect to the ear-to-ear axis). The ICNIRP and IEEE-2005 standards propose identical reference levels at both 2.44 and 5.8 GHz, which correspond to 10 W/m^2 for public exposure. The respective limits for controlled environments are 81.333 and 100 W/m^2 in the case of IEEE-2005,

Table 3. Temperature rise (overall, brain, eyes) in °C, for exposure to plane waves featuring maximum power densities.

Case	2.44 GHz	5.8 GHz
ICNIRP (GP*), IEEE (AL*)	0.091, 0.026, 0.052	0.110, 0.025, 0.047
ICNIRP (occupational)	0.451, 0.130, 0.257	0.551, 0.123, 0.236
IEEE (controlled)	0.739, 0.212, 0.419	1.101, 0.246, 0.471

* GP = General Public, AL = Action Level

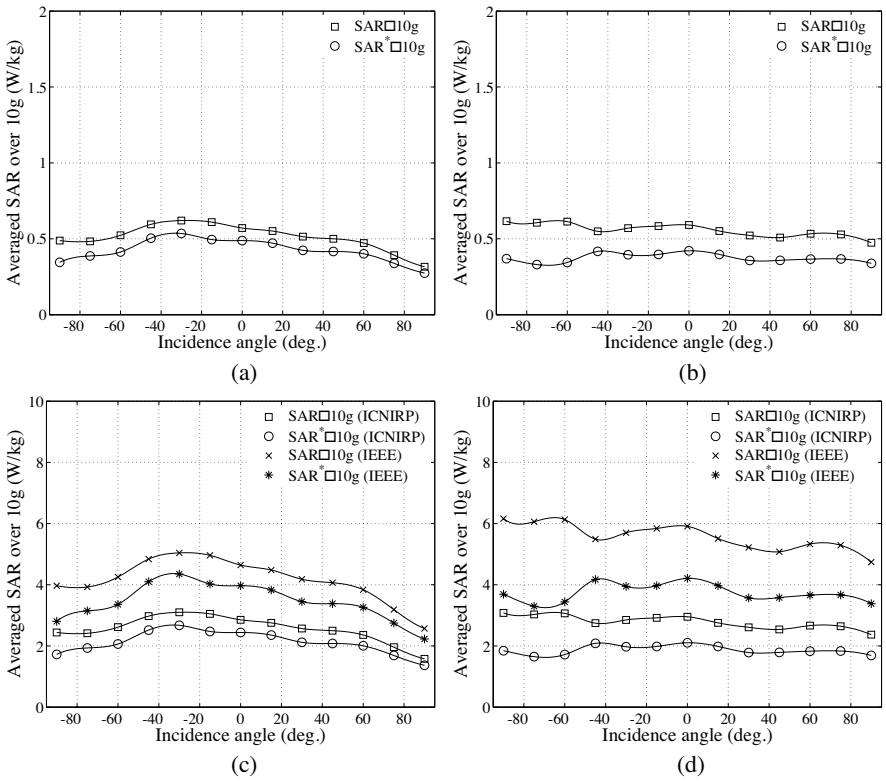

Figure 8. SAR-10g versus incidence angle, for plane-wave illumination: (a) (2.44 GHz, 10 W/m^2), (b) (5.8 GHz, 10 W/m^2), (c) (2.44 GHz, 50 and 81.333 W/m^2), (d) (5.8 GHz, 50 and 100 W/m^2).

while ICNIRP proposes 50 W/m^2 for occupational exposure in both bands (recall that the 10 W/kg SAR-10g limit applies in the latter cases). Figure 8 exhibits the calculated SAR-10g and SAR*-10g values as a function of the incidence angle, considering the aforementioned worst-case scenarios. Although no violation of the safety limits is observed, quite significant values can be detected: for instance, SAR-10g reaches 5.042 W/kg at 2.44 GHz and 6.16 W/kg at 5.8 GHz, in the case of the IEEE-2005 standard. Note that the SAR*-10g indicator provides approximately 21.6% and 32% lower values at the two bands, respectively. Finally, the overall temperature elevations, as well as those occurring in the brain and the eyes, are given in Table 3. Compared to the eyes, brain tissues appear less susceptible to thermal changes.

4. CONCLUSION

We have presented a multidisciplinary numerical study of human exposure to radio-frequency EM fields. Simulations with mobile phones revealed SAR-10g indices lower than 1 W/kg and temperature changes of the order of 0.1°C. Examination of the near-field exposure to dipole antennas allowed us to propose general models correlating the dissipated power and the thermal effects, which enabled further predictions of the expected temperature elevations at marginal exposures. Also, extreme cases considering maximum incident power densities indicated compliance with the standards and stimulated various interesting observations. Future extensions of this work will incorporate the more general investigation of full-body exposure, as well as other types of transmitting sources (such as on-body antennas or implanted devices).

REFERENCES

1. Kang, X. K., L. W. Li, M. S. Leong, and P. S. Kooi, "A spheroidal vector wave function analysis of field and SAR distributions in a dielectric prolate spheroidal human head model," *Progress In Electromagnetics Research*, PIER 22, 149–179, 1999.
2. Li, L. W., M. S. Leong, P. S. Kooi, and T. S. Yeo, "Specific absorption rates in human head due to handset antennas: A comparative study using FDTD method," *J. of Electromagn. Waves and Appl.*, Vol. 14, 987–1000, 2000.
3. Gandhi, O. P., Q.-X. Li, and G. Kang, "Temperature rise for the human head for cellular telephones and for peak SARs prescribed in safety guidelines," *IEEE Trans. Microw. Theory Tech.*, Vol. 49, 1607–1613, 2001.
4. Kang, X. K., L. W. Li, M. S. Leong, and P. S. Kooi, "A method of moments study of SAR inside spheroidal human head and current distribution along handset wire antennas," *J. of Electromagn. Waves and Appl.*, Vol. 15, 61–75, 2001.
5. Yioultsis, T. V., T. I. Kosmanis, E. P. Kosmidou, T. T. Zygiridis, N. V. Kantartzis, T. D. Xenos, and T. D. Tsiboukis, "A comparative study of the biological effects of various mobile phone and wireless LAN antennas," *IEEE Trans. Magn.*, Vol. 38, 777–780, 2002.
6. Hirata, A. and T. Shiozawa, "Correlation of maximum temperature increase and peak SAR in the human head due to handset

antennas," *IEEE Trans. Microw. Theory Tech.*, Vol. 51, 1834–1841, 2003.

7. Wang, J., O. Fujiwara, S. Watanabe, and Y. Yamanaka, "Computation with a parallel FDTD system of human-body effect on electromagnetic absorption for portable telephones," *IEEE Trans. Microw. Theory Tech.*, Vol. 52, 53–58, 2004.
8. Whittow, W. G. and R. M. Edwards, "A study of changes to specific absorption rates in the human eye close to perfectly conducting spectacles within the radio frequency range 1.5 to 3.0 GHz," *IEEE Trans. Antennas Propag.*, Vol. 52, 3207–3212, 2004.
9. Ibrahiem, A., C. Dale, W. Tabbara, and J. Wiart, "Analysis of the temperature increase linked to the power induced by RF source," *Progress In Electromagnetics Research*, PIER 52, 23–46, 2005.
10. Kiminami, K., A. Hirata, Y. Horii, and T. Shiozawa, "A study on human body modeling for the mobile terminal antenna design at 400 MHz band," *J. of Electromagn. Waves and Appl.*, Vol. 19, 671–687, 2005.
11. Hadjem, A., D. Lautru, C. Dale, M. F. Wong, V. F. Hanna, and J. Wiart, "Study of specific absorption rate (SAR) induced in two child head models and in adult heads using mobile phones," *IEEE Trans. Microw. Theory Tech.* Vol. 53, 4–11, 2005.
12. Yoshida, K., A. Hirata, Z. Kawasaki, and T. Shiozawa, "Human head modeling for handset antenna design at 5 GHz band," *J. of Electromagn. Waves and Appl.*, Vol. 19, 401–411, 2005.
13. Li, Q.-X. and O. P. Gandhi, "Thermal implications of the new relaxed IEEE RF safety standard for head exposures to cellular telephones at 835 and 1900 MHz," *IEEE Trans. Microw. Theory Tech.*, Vol. 54, 3146–3154, 2006.
14. Hirata, A., M. Fujimoto, T. Asano, J. Wang, O. Fujiwara, and T. Shiozawa, "Correlation between maximum temperature increase and peak SAR with different average schemes and masses," *IEEE Trans. Electromagn. Compat.*, Vol. 48, 569–578, 2006.
15. Kuo, L.-C., Y.-C. Kan, and H.-R. Chuang, "Analysis of a 900/1800-MHz dual-band gap loop antenna on a handset with proximate head and hand model," *J. of Electromagn. Waves and Appl.*, Vol. 21, 107–122, 2007.
16. Togashi, T., T. Nagaoka, S. Kikuchi, K. Saito, S. Watanabe, M. Takahashi, and K. Itoh, "FDTD calculations of specific absorption rate in fetus caused by electromagnetic waves from mobile radio terminal using pregnant woman model," *IEEE Trans.*

Microw. Theory Tech., Vol. 56, 554–559, 2008.

17. ICNIRP, "Guidelines for limiting exposure to time-varying electric, magnetic, and electromagnetic fields (up to 300 GHz)," *Health Phys.*, Vol. 74, 494–522, 1998.
18. *IEEE Standard for Safety Levels with Respect to Human Exposure to Radio Frequency Electromagnetic Fields, 3 kHz to 300 GHz*, IEEE Standard C95.1-2005, 2005 Edition.
19. *IEEE Standard for Safety Levels with Respect to Human Exposure to Radio Frequency Electromagnetic Fields, 3 kHz to 300 GHz*, IEEE Standard C95.1-1999, 1999 Edition.
20. Taflove, A. and S. C. Hagness, *Computational Electrodynamics: The Finite-Difference Time-Domain Method*, Artech House, Norwood, MA, 2005.
21. ftp://starview.brooks.af.mil/EMF/dosimetry_models
22. Gabriel, S., R. W. Lau, and C. Gabriel, "The dielectric properties of biological tissues: III. Parametric models for the dielectric spectrum of tissues," *Phys. Med. Biol.*, Vol. 41, 2271–2293, 1996.
23. Berenger, J.-P., "A perfectly matched layer for the absorption of electromagnetic waves," *J. Comp. Phys.*, Vol. 114, 185–200, 1994.
24. Ismail, N. H. and A. T. Ibrahim, "Temperature distribution in the human brain during ultrasound hyperthermia," *J. of Electromagn. Waves and Appl.*, Vol. 16, 803–811, 2002.
25. Kivekas, O., J. Ollikainen. T. Lehtiniemi, and P. Vainikainen, "Bandwidth, SAR, and efficiency of internal mobile phone antennas," *IEEE Trans. Electromag. Compat.*, Vol. 46, 71–85, 2004.